BJ www.biochemj.org

Biochem. J. (2010) **430**, 487–495 (Printed in Great Britain) doi:10.1042/BJ20100289

Determinants of activity in glutaredoxins: an *in vitro* evolved Grx1-like variant of *Escherichia coli* Grx3

Tobias H. ELGÁN*†[1], Anne-Gaëlle PLANSON‡[2], Jon BECKWITH‡, Peter GÜNTERT§‖¶ and Kurt D. BERNDT*†

*Department of Biosciences and Nutrition, Karolinska Institutet, NOVUM, S-141 57 Huddinge, Sweden, †School of Life Sciences, Södertörns Högskola, S-141 89 Huddinge, Sweden, ‡Department of Microbiology and Molecular Genetics, Harvard Medical School, Boston, MA 02115, U.S.A., §Tatsuo Miyazawa Memorial Program, RIKEN Genomic Sciences Center, 1-7-22 Suehiro-cho, Tsurumi, Yokohama 230-0045, Japan, ‖Institute of Biophysical Chemistry and Frankfurt Institute for Advanced Studies, Max-von-Laue-Straße 9, Goethe-University Frankfurt, 60438 Frankfurt am Main, Germany, and ¶Graduate School of Science, Tokyo Metropolitan University, 1-1 Minami-ohsawa, Hachioji, Tokyo 192-0397, Japan

The *Escherichia coli* glutaredoxins 1 and 3 (Grx1 and Grx3) are structurally similar (37 % sequence identity), yet have different activities *in vivo*. Unlike Grx3, Grx1 efficiently reduces protein disulfides in proteins such as RR (ribonucleotide reductase), whereas it is poor at reducing S-glutathionylated proteins. An *E. coli* strain lacking genes encoding thioredoxins 1 and 2 and Grx1 is not viable on either rich or minimal medium; however, a M43V mutation in Grx3 restores growth under these conditions and results in a Grx1-like protein [Ortenberg, Gon, Porat and Beckwith (2004) Proc. Natl. Acad. Sci. U.S.A. **101**, 7439–7944]. To uncover the structural basis of this change in activity, we have compared wild-type and mutant Grx3 using CD and NMR spectroscopy. Ligand-induced stability measurements demonstrate that the Grx3(M43V/C65Y) mutant has acquired affinity for RR. Far-UV CD spectra reveal no significant differences, but differences are observed in the near-UV region indicative of tertiary structural changes. NMR ^{1}H-^{15}N HSQC (heteronuclear single quantum coherence) spectra show that approximately half of the 82 residues experience significant ($\Delta\delta > 0.03$ p.p.m.) chemical shift deviations in the mutant, including nine residues experiencing extensive ($\Delta\delta \geqslant 0.15$ p.p.m.) deviations. To test whether the M43V mutation alters dynamic properties of Grx3, H/D (hydrogen/deuterium) exchange experiments were performed demonstrating that the rate at which backbone amides exchange protons with the solvent is dramatically enhanced in the mutant, particularly in the core of the protein. These data suggest that the Grx1-like activity of the Grx3(M43V/C65Y) mutant may be explained by enhanced intrinsic motion allowing for increased specificity towards larger substrates such as RR.

Key words: chemical shift, glutaredoxin (Grx), hydrogen/deuterium exchange, ligand-induced stability, NMR, ribonucleotide reductase.

INTRODUCTION

The Grxs (glutaredoxins) are ubiquitous enzymes found in virtually all life forms from plants and viruses to humans. They are members of the Trx (thioredoxin) superfamily characterized by a common tertiary structure, the Trx fold [1], and a highly conserved -C-X-X-(C/S)- active site motif [2]. By utilizing the redox properties of these active site cysteine residues, the Grxs participate in reversible disulfide bond formation thereby protecting cells against oxidative stress [3], and having a profound impact on cellular functions, affecting, for example, enzymatic activity and regulatory pathways [4,5]. It has been proposed that the Grxs exert their catalytic activity via a monothiol pathway in which only the N-terminal active site cysteine residue is required to reversibly reduce glutathione-mixed disulfides and via a dithiol pathway requiring both active site cysteine residues to reduce low molecular mass and protein disulfides [6].

Four Grxs have been identified in the *Escherichia coli* genome [7]. The highly abundant 24 kDa Grx2 and the 13 kDa Grx4 are atypical Grxs in the sense that the former has an additional structural domain making it similar to the glutathione transferases, whereas the latter has a highly conserved monothiol -C-G-F-S- active site sequence [2]. Grx1 and Grx3 (10 and 9 kDa respectively) are both prototypical Grxs containing the classical Grx -C-P-Y-C- active site sequence and are structurally very similar [6,8] as indicated by their 37 % sequence identity. It has been observed that these Grxs have both overlapping and distinct activities. Although both Grx1 and Grx3 are excellent reductants of glutathione–protein mixed disulfides [9,10], only Grx1 is capable of efficiently reducing the essential enzyme RR (ribonucleotide reductase) [10,11] and PAPS (3′-phosphoadenylylsulfate) reductase [12].

A previous study by Ortenberg et al. [13] on the differences in substrate specificities among the Grxs focused on the *E. coli* proteins Grx1 and Grx3. Using a PCR-prone mutagenesis approach within an *E. coli* strain missing Trx1, Trx2 and Grx1 (all capable of reducing RR), a single site point mutant form of Grx3, which restores bacterial growth, was repeatedly identified. It was found that the affected residue position Met^{43}, located outside the active site, was mutated into an isoleucine, leucine or valine residue; the latter having the most prominent effect. Furthermore, Porat et al. [14] characterized the Grx3(M43V) mutant biochemically and by molecular dynamics simulations. These results showed that: (i) the altered protein gained a 7-fold

Abbreviations used: DTT, dithiothreitol; ESI–MS, electrospray ionization MS; Grx, glutaredoxin; Grx–SG, Grx-glutathione mixed disulfide; ΔG_{H_2O}, Gibbs free energy in absence of denaturant; $\Delta\Delta G_{H_2O}$, difference in conformational stability between two proteins; H/D, hydrogen/deuterium; HSQC, heteronuclear single quantum coherence; IPTG, isopropyl β-D-thiogalactoside; LB, Luria–Bertani; 2Me, 2-mercaptoethanol; RP, reverse phase; RR, ribonucleotide reductase; RRp, *Escherichia coli* RR peptide comprising residues 1737–1761 (C754S); Trx, thioredoxin.

[1] To whom correspondence should be addressed at the present address: STAD, Stockholm Centre for Psychiatric Research and Education, Department of Clinical Neuroscience, Stockholm County Council Health Care Provision and Karolinska Institutet, Box 6031, S-102 31 Stockholm, Sweden (email tobias.elgan@sll.se).

[2] Present address: Institut de Biologie et Technologies-Saclay iBiTecs CEA-Saclay, Bat 142 91191 Gif-sur-Yvette, France

increase in V_{max} towards reducing RR while leaving the K_m value unaffected; (ii) the N-terminal active site cysteine residue of the mutant has a 1.1 unit lower pK_a value; (iii) the redox potential of the active site cysteine residues is 11 mV more reducing in the mutant protein; and (iv) molecular dynamics simulations demonstrated that the structure of the mutant did not differ from the wild-type protein. Altogether, it was concluded that the mutation affects the activity of Grx3 by reducing the N-terminal active site pK_a value, and therefore lowers the redox potential.

Previous studies [14–16] have suggested that at least part of the observed difference in activity between Grx1 and Grx3 is related to a greater flexibility in the former. To test this hypothesis and gain insight into the acquired Grx1-like activity caused by the M43V mutation in Grx3, we have investigated structural and dynamic properties of this mutant. By using CD and NMR spectroscopy, we have investigated structural and dynamic changes caused by the M43V mutation in Grx3 which has conferred the Grx1-like activity to the Grx3 enzyme.

EXPERIMENTAL

Protein expression and purification

Mutant *grxC* genes [encoding *E. coli* Grx3(C65Y) and the C14S/C65Y version] inserted in pET24d (Novagen) vectors and *grxA* genes (encoding wild-type *E. coli* Grx1 and the C14S mutant) inserted in pET101D-TOPO vectors (Invitrogen) were available within our laboratory. The M43V mutation was introduced into the two mutant *grxC* genes using the QuikChange mutagenesis kit (Stratagene) and the following primers: 5′-GCCAAGCGTGAAGAGGTGATCAAACGCAGCGG-3′ and 5′-CCGCTGCGTTTGATCACCTCTTCACGCTTGGC-3′. The vector constructs were transformed into *E. coli* BL21 Star (DE3) cells (Invitrogen) using standard procedures. The expression, purification and characterization of the Grx1 and Grx3 constructs were performed as described previously [17].

For the NMR measurements, uniformly ^{15}N-labelled Grx3 in both C65Y and M43V/C65Y mutant forms and a ^{15}N/^{13}C-double-labelled M43V/C65Y mutant sample were prepared using the method of Marley et al. [18]. Briefly, a starter culture was grown over night in LB (Luria–Bertani) medium containing kanamycin (50 μg/ml) at 37 °C and then diluted into 2 litres of LB medium. When the A_{600} reached ~0.8, cells were harvested by centrifugation for 20 min at 7000 ***g***, washed with 2 litres of M9 minimal medium, centrifuged, and then resuspended in M9 medium enriched with [^{13}C]glucose (or natural abundance glucose) and [^{15}N]ammonium sulfate. The culture was grown at 37 °C for 1 h and then induced with IPTG (isopropyl β-D-thiogalactoside; 1 mM final concentration). The culture was incubated overnight at 37 °C and then harvested by centrifugation. Protein concentrations were determined by UV absorbance at 280 nm using the following molar absorbance coefficients [19]: 5120 $M^{-1} \cdot cm^{-1}$ for all Grx3 variants (5240 $M^{-1} \cdot cm^{-1}$ for the corresponding mixed disulfides) and 10810 $M^{-1} \cdot cm^{-1}$ for the Grx1 variants (10930 $M^{-1} \cdot cm^{-1}$ for mixed disulfides).

In vivo activity of Grx3(M43V/C65Y)

The *in vivo* activity of the *E. coli* Grx3(M43V) and M43V/C65Y mutants towards RR was determined as described by Ortenberg et al. [13]. Briefly, a pAG10 plasmid encoding *E. coli* Grx3(M43V/C65Y) was constructed by site-directed mutagenesis (QuikChange mutagenesis kit, Stratagene) from a pRO2 plasmid template carrying the *grxC(M43V)* gene encoding Grx3(M43V) [13] under the control of a lacUV5 promoter and tetracycline resistance as a selectable marker. For this purpose, the following primers were used: 5′-GCACATTGGC-GGCTATGATGACTTGTAC-3′ and 5′-GTACAAGTCATCATA-GCCGCCAATGTGC-3′. The pRO2 and the resulting pAG10 plasmids were transformed into *E. coli* bacteria (strain RO36, DHB4 Δ*trxA* Δ*trxC grxA::kan nrdH::spc*/pBAD18-*trxC*) and transferred to separate NZ-amine plates supplemented with 15 μg/ml tetracycline and 0.2 % arabinose to induce Trx2 expression. Selected colonies were picked and transferred to NZ plates supplemented with 0.2 % glucose (to repress Trx2 expression) in the absence and presence of 1 mM IPTG required for the expression of the Grx3 mutant. In the latter condition, only the expression of a Grx3 mutant that is able to reduce RR will be able to restore bacterial growth.

Ligand-induced conformational stability measurements using CD spectroscopy

Crude RRp (RR peptide, residues 737–761 from C754S mutant *E. coli* RR [20]) was purchased (Keck Biotechnology Resource Center) in the reduced state and purified by RP (reverse phase)-HPLC (Chemstation 1100, Agilent Technologies) using a C_{18} semi-preparative column (218TPB510, Vydac) by applying a gradient from 10 to 40 % acetonitrile/water (0.1 % trifluoroacetic acid) over 45 min. The peptide was dissolved in distilled water and freeze-dried several times in a speed-vac (Savant), and finally dissolved in 50 mM phosphate, 50 μM EDTA buffer at pH 7.0. RRp–2Me (2-mercaptoethanol) mixed disulfide was prepared by incubating reduced RRp with a 100-fold molar excess of 2-hydroxyethyl disulfide (Aldrich) overnight and HPLC purification as above followed by ESI–MS (electrospray ionization MS) analysis (Finnigan MAT LCQ).

Grx–RRp mixed disulfides were prepared by incubating reduced protein (typically at a concentration of ~0.2 mM) overnight at 4 °C with a 20-fold molar excess of RRp–2Me mixed disulfide followed by gel filtration (PD-10, GE Healthcare). Grx–RRp mixed disulfide formation was confirmed by analytical RP-HPLC followed by ESI–MS as above. The preparation of the Grx–SG and Grx–2Me mixed disulfides have been described elsewhere [17].

Conformational stabilities of proteins in their reduced and corresponding mixed disulfide complexes with RRp, glutathione and 2Me were measured by semi-automated unfolding experiments using urea (ICN Biomedicals) and monitored using an Aviv 202 spectropolarimeter (Aviv Biomedical) equipped with a two-syringe pipetting robot (Microlab 500, Hamilton). The protein (mixed disulfide) concentrations ranged from 2.5 to 3.4 μM and experiments were performed at 25 °C using the same buffer as above. The unfolding reactions were monitored at 222 nm as the urea concentration was increased in 0.125 M steps into a stirred quartz cuvette with 1 cm pathlength. Samples were allowed to equilibrate for 7 min after each addition of urea followed by data collection for 30 s.

Assuming that the protein unfolding reaction in the presence of a denaturant, D, is a reversible two-state process between the folded (f) and unfolded (u) forms and that the unfolding free energy (ΔG^{Unfold}) is a linear function of the denaturant concentration [D] and the unfolding free energy in the absence of denaturant ($\Delta G^{Unfold}_{H_2O}$), an equation for the experimental observable (y_{obs}) can be derived as described previously [21,22]:

$$y_{obs} = \frac{(y_f + m_f[D]) + (y_u + m_u[D]) \cdot \exp\left\{\frac{m_{trans}[D] + \Delta G^{Unfold}_{H_2O}}{RT}\right\}}{1 + \exp\left\{\frac{m_{trans}[D] + \Delta G^{Unfold}_{H_2O}}{RT}\right\}} \quad (1)$$

where y_{obs} is the observed CD signal at 222 nm, m_{trans} is the denaturant dependency of the measured free energy changes of unfolding (ΔG^{Unfold}); y_f and y_u are the observed values of the CD signal of fully folded and unfolded forms respectively; m_f and m_u refer to the slopes of the linear pre- and post-transition regions respectively; R is the gas constant ($1.986\ cal \cdot K^{-1} \cdot mol^{-1}$); and T is the temperature is Kelvin. Raw data from the urea titration experiments were fitted to eqn (1) using the Levenberg–Marquardt, non-linear least-squares regression routine in the Igor Pro software package (WaveMetrics). Values describing the conformational stabilities are reported in terms of the folding reaction using the following relationship $\Delta G^{fold}_{H_2O} = -\Delta G^{Unfold}_{H_2O}$.

Redox potential determination using thermodynamic linkage

Reduced Grx3(M43V/C65Y) was prepared as above. The oxidized form was obtained by incubating previously reduced protein in a 50-fold molar excess of GSSG for 1 h followed by gel filtration (as above). The conformational stability and subsequent analysis of reduced and oxidized Grx3(M43V/C65Y) was determined by urea unfolding monitored by CD spectroscopy as above. Subsequent calculation of the redox potential was performed as described previously [2,23] using the thermodynamic linkage relationship between the stability of a disulfide bond to the stability of a protein containing it [24].

CD wavelength scans

CD spectra of the proteins in their respective reduced states were collected using an Aviv 62 DS spectropolarimeter (Aviv Biomedical). The reduced forms of the proteins were prepared by adding a 50-fold molar excess of DTT (dithiothreitol), which was removed after 1 h by gel filtration (NAP-5, GE Healthcare). Measurements were performed in degassed 50 mM potassium phosphate buffer, pH 7.0, with 50 μM EDTA. Far-UV CD measurements were performed in a 0.01 cm quartz cuvette (Hellma) between 260 and 180 nm for 12 s every 1.0 nm using a bandwidth of 1.5 nm. Data were converted into mean residue molar circular dichroism ($\Delta\varepsilon$) using the relationship $\Delta\varepsilon = [\Theta]_{MRW}/3298$, where $[\Theta]_{MRW}$ is the mean residue molar ellipticity. The near-UV CD spectra were measured in a 1.0 cm quartz cuvette (Hellma) between 340 and 250 nm. Data were collected for 8 s every 0.3 nm using a bandwidth of 0.3 nm. Data from the near-UV scans, reported as molar ellipticity [Θ], were smoothed using a polynomial fitting routine in the Igor Pro software package. The protein concentrations were $\sim$165 μM for all far-UV CD measurements and $\sim$140 μM for all near-UV measurements.

NMR spectroscopy

All NMR measurements were performed on a Varian Inova 500 MHz spectrometer (Varian) at 25 °C using protein concentrations between 1.5 and 3 mM in degassed 50 mM potassium phosphate buffer, pH 6.6, 50 μM EDTA and 5 mM DTT containing 5 % ^2H_2O. Sequence-specific resonance assignment of the M43V/C65Y mutant was achieved by using a ^1H-^{15}N HSQC (heteronuclear single quantum coherence) and a set of triple resonance experiments [25] which included HNCA, HN(CO)CA, HNCO, HN(CA)CO, CBCANH, and CBCA(CO)NH. All NMR spectra were processed with the NMRPipe software package [26] and analysed using the NMRViewJ software (One Moon Scientific). The resulting peak lists were used as input for automated resonance assignment using the GARANT program [27].

Uniformly ^{15}N-labelled C65Y and M43V/C65Y mutant Grx3 proteins were freeze-dried as described above. Time correlated H/D (hydrogen/deuterium) exchange experiments [28] of exchangeable protons were initiated by the addition of ^2H_2O to the freeze-dried proteins. The H/D-exchange reaction was followed by collecting a series of ^{15}N HSQC spectra as a function of time. A total of 60 spectra for a period of 28.2 days and 26 spectra during 6.2 h were collected for the C65Y and the M43V/C65Y mutant proteins respectively, until all amide proton peaks had disappeared. The spectra were processed as above and the resulting peak areas determined using the XEASY software [29]. Pseudo first-order rate constants were calculated by fitting the resulting data points to a first-order equation using the Igor Pro software package.

RESULTS AND DISCUSSION

Cys^{65} of Grx3 has no apparent effect on the reducing ability of RR *in vivo*

Apart from its two active site cysteine residues, Grx3 has an additional cysteine residue (Cys^{65}) located outside the active site which has been found to have homologous counterparts in all but one Grx subgroup (based on the human Grxs) [2]. This residue has been observed to form intermolecular disulfides *in vitro*, thereby producing homodimers or mixed disulfides [23], complicating structural and functional studies of the active site. This behaviour can be avoided by using a C65Y mutant which has essentially identical activity with the wild-type protein *in vitro* [8] and has therefore been used extensively in other studies [8,17,23,30]. Until the present study, the *in vivo* significance of this residue remained uncertain, although it had been demonstrated that a homologous cysteine residue in the monothiol yeast Grx5 rescued a dithiol-like mechanism (involving two Grx cysteine residues) [31]. To test whether the Cys^{65} residue has an impact on the *in vivo* reduction of RR [13], Grx3(M43V) and Grx3(M43V/C65Y) mutants were expressed in *E. coli* that lack the genes encoding proteins capable of reducing RR. The ability of the Grx3(M43V/C65Y) mutant to restore bacterial growth to the same extent as the M43V mutant (results not shown) demonstrates that the C65Y mutation does not affect the *in vivo* activity, as determined by these phenotypes, and justifies the usage of the C65Y version of Grx3.

The following Grx3 variants were used in the present study: C65Y (sometimes referred to as wild-type), M43V/C65Y, C14S/C65Y and C14S/M43V/C65Y.

The Grx3(M43V/C65Y) mutant has increased affinity for RR

The free energy of binding of a ligand to a protein gives rise to a change in conformational stability ($\Delta G^{Fold}_{H_2O}$) with respect to the unbound form. Depending on how well a ligand interacts with a protein non-covalently, a ligand can either have a stabilizing or destabilizing effect on the protein–ligand complex. This ligand-induced (de)stabilization ($\Delta\Delta G$) is a measure of ligand affinity, and has proven to be a useful approach to dissect specificity as individual interactions between a protein and a ligand can be quantified using a set of ligand analogues [17]. The approach is particularly appropriate for the Grxs, since catalysis naturally proceeds via a transiently stable covalent mixed disulfide which can be trapped using a C-terminal active site cysteine-to-serine variant. A recent study from our laboratory on Grx3 substrate specificity demonstrated that, although the tripeptide glutathione (γ-Glu-Cys-Gly) has a stabilizing effect by 0.50 ± 0.13 kcal $\cdot$ mol^{-1} (1 kcal $\approx$ 4.184 kJ) upon Grx3 mixed disulfide formation, it does not have a significant impact

Table 1 Parameters (± S.D.) obtained from ligand-induced stability measurements using urea unfolding monitored by CD at 222 nm

The unfolding curves of non-bound and RRp-mixed disulfide forms of Grx1 and Grx3 (both wild-type and M43V/C65Y mutant) were fitted to eqn (1) by non-linear regression analysis. The parameters from the unfolding of reduced and oxidized wild-type Grx3 M43V/C65Y, used for redox potential determination using thermodynamic linkage, are also included. Here, $\Delta\Delta G_1$ is the free energy contribution upon ligand binding or disulfide formation relative to non-bound/reduced Grx1 and Grx3; $\Delta\Delta G_2$ is the free energy contribution of non-covalent interactions between ligand and protein; $[\text{Urea}]_{1/2}$ is the midpoint of the urea unfolding curve; m_{trans} is the slope in the transition region of the unfolding curve; n.a., not applicable.

Protein–(mixed disulfide)	$\Delta G^{\text{Fold}}_{H_2O}$ (kcal · mol^{-1})	$\Delta\Delta G_1$ (kcal · mol^{-1})	$\Delta\Delta G_2$ (kcal · mol^{-1})	$[\text{Urea}]_{1/2}$ (M)	m_{trans} (kcal · mol^{-1} · M^{-1})
Grx3(C14S) non-bound	−4.74 ± 0.12	n.a.	−2.61 ± 0.15	3.85 ± 0.15	−1.23 ± 0.03
Grx3(C14S)–2Me*	−2.13 ± 0.09	2.61 ± 0.15	n.a.	1.38 ± 0.07	−1.54 ± 0.04
Grx3(C14S)–RRp	−4.70 ± 0.14	0.04 ± 0.18	−2.57 ± 0.17	3.79 ± 0.15	−1.24 ± 0.04
Grx3(C14S)–SG*	−5.20 ± 0.10	−0.46 ± 0.16	−3.07 ± 0.13	5.42 ± 0.15	−0.96 ± 0.02
Grx3(C14S/M43V/C65Y) non-bound	−2.06 ± 0.08	n.a.	−2.68 ± 0.08	1.55 ± 0.15	−1.33 ± 0.03
Grx3(C14S/M43V/C65Y)–2Me	0.62 ± 0.01	2.68 ± 0.08	n.a.	−0.37 ± 0.12	−1.66 ± 0.07
Grx3(C14S/M43V/C65Y)–RRp	−3.57 ± 0.09	−1.51 ± 0.12	−4.19 ± 0.09	2.95 ± 0.10	−1.21 ± 0.03
Grx3(C14S/M43V/C65Y)–SG	−3.36 ± 0.06	−1.30 ± 0.10	−3.98 ± 0.06	2.42 ± 0.06	−1.39 ± 0.02
Grx1(C14S) non-bound	−3.60 ± 0.12	n.a.	−2.82 ± 0.12	2.90 ± 0.13	−1.24 ± 0.04
Grx1(C14S)–2Me	−0.78 ± 0.01	2.82 ± 0.12	n.a.	0.93 ± 0.03	−0.84 ± 0.02
Grx1(C14S)–RRp	−5.50 ± 0.17	−1.90 ± 0.21	−4.72 ± 0.17	5.85 ± 0.26	−0.94 ± 0.03
Grx1(C14S)–SG*	−3.63 ± 0.14	−0.03 ± 0.18	−2.85 ± 0.18	3.99 ± 0.23	−0.91 ± 0.04
Grx3(M43V/C65Y) reduced	−3.01 ± 0.04	n.a.	n.a.	2.43 ± 0.07	−1.24 ± 0.03
Grx3(M43V/C65Y) oxidized	−2.55 ± 0.06	0.46 ± 0.07	n.a.	1.81 ± 0.05	−1.41 ± 0.02

*Values taken from [17].

upon complex formation with Grx1(Table 1) [17]. This result correlates with the enzymatic activities of these proteins, since Grx3 is more efficient than Grx1 at reducing glutathione-mixed disulfides [8,11]. That thermodynamic properties can be used within the Grx family as an indicator of enzymatic activity has been demonstrated previously [32]. However, as pointed out by Saaranen et al. [32], comparisons between thermodynamic and kinetic properties should be made with caution as these properties are not readily interconvertible. Nevertheless, since previous studies have indicated that the Grx3(M43V/C65Y) mutant acquired an enhanced ability to reduce RR, it is feasible to use ligand-induced stability to test for alterations in affinity.

In the present study, active site C14S variants of wild-type and mutant Grx1 and Grx3 together with a 25-residue peptide from RR (RRp, the C1754S mutant of residues 1737–1761) [16] was used. The RRp peptide has been demonstrated to bind to Grx1 in a specific manner [16], thereby mimicking the intermediate Grx–RR mixed disulfide form. After the formation of 1:1 mixed disulfide complexes between the different Grx variants and the RRp peptide, the conformational stabilities of unbound and RRp-peptide-bound forms were determined by urea unfolding monitored by CD spectroscopy. As shown in Figure 1 and Table 1, Grx1(C14S) is stabilized by ($\Delta\Delta G_1$) 1.90 ± 0.21 kcal · mol^{-1} upon mixed disulfide formation with the RRp peptide. The effect exerted by the M43V mutation on Grx3 affinity to RR is apparent as the RRp peptide has no significant impact on the stability of the corresponding Grx3(C14S) complex ($\Delta\Delta G_1 = 0.04 \pm 0.18$ kcal · mol^{-1}), whereas the Grx3(C14S/M43V/C65Y) mutant is stabilized by ($\Delta\Delta G_1$) 1.51 ± 0.12 kcal · mol^{-1} upon mixed disulfide formation with RRp. Furthermore, by comparing the Grx mixed disulfides with glutathione and the RRp peptide to the corresponding 2Me-mixed disulfides, it is possible to quantify how much all interactions between the protein and ligand are worth ($\Delta\Delta G_2$). Thus it is shown that, although the total interactions between glutathione and Grx3(C14S/C65Y) are worth ($\Delta\Delta G_2$) -3.07 ± 0.13 kcal · mol^{-1} (Table 1), the interactions between the same protein and the RRp-peptide amounts to -2.57 ± 0.17 kcal · mol^{-1}. Thus the Grx3(C14S/C65Y) protein makes more

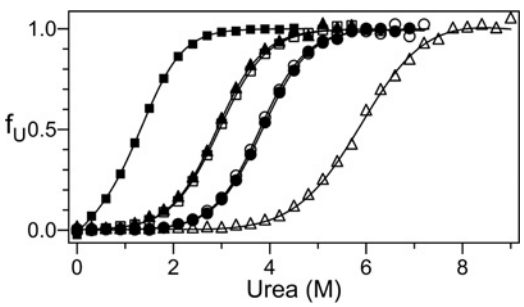

Figure 1 Ligand-induced stability effects upon Grx1 and Grx3 (wild-type and M43V/C65Y) binding to RR B1-peptide

Urea unfolding reactions monitored by CD spectroscopy at 222 nm of non-bound and RR B1 peptide (RRp)-bound forms of Grx1 and Grx3, represented by the fraction of unfolded protein (f_u): Grx1(C14S) in non-bound (▲) and bound (△) forms, Grx3(C14S) in non-bound (●) and bound (○) forms, and Grx3(C14S/M43V/C65Y) in non-bound (■) and bound (□) forms. The data were fitted (solid lines) to eqn (1) by non-linear regression analysis.

favourable interactions to glutathione relative to the RRp peptide (by 0.5 ± 0.21 kcal · mol^{-1}). Making the same analysis with the corresponding Grx1(C14S) and Grx3(C14S/M43V/C65Y) mixed disulfides with glutathione and RRp reveals that, unlike the Grx3(C14S/C65Y) protein, these two proteins make more favourable interactions with the RRp-peptide by 1.87 ± 0.25 kcal · mol^{-1} ($\Delta\Delta G_2 = -4.72 \pm 0.17$ compared with -2.85 ± 0.18 kcal · mol^{-1}) and 0.21 ± 0.11 kcal · mol^{-1} ($\Delta\Delta G_2 = -4.19 \pm 0.09$ compared with -3.98 ± 0.06 kcal · mol^{-1}) respectively. It then appears as if the M43V mutation has altered the binding properties of the Grx3 protein as this variant makes stronger interactions with the RRp-peptide and less prominent interactions with glutathione, indicating less activity with regards to reducing S-glutathionylated proteins [17].

The results presented above, however, do not correlate with previous findings. Assuming Michaelis–Menten kinetics, Porat et al. [14] reported that an improved $V_{\max}$ rather than K_m was responsible for the Grx1-like behaviour of the Grx3(M43V) mutant.

What is then the reason for the discrepancy between these results? The K_m value represents an apparent dissociation constant which characterizes the total binding event based on Michaelis–Menten kinetics, including all bound forms of the substrate. When using the K_m value as a measure of affinity, it is assumed that the rate-limiting step is the product formation and that any intermediary enzyme–product complex is ignored since dissociation of this complex into enzyme and product is fast. However, it has been demonstrated previously that Grxs have a tendency to form a transiently stable substrate mixed disulfide [2,23], which makes the interpretation of K_m values in the case of mixed disulfides complex. It is then possible that the previously reported K_m values and the results from the affinity measurement reported in the present study are not comparable since they probe different phenomena (i.e. product formation and protein–substrate binding).

The reducing ability of the Grx3(M43V/C65Y) mutant is improved

It has been reported that the redox potential ($E^{o\prime}$) of the Grx3(M43V) mutant was lowered by 11 mV relative to the wild-type protein (−203 mV and −192 mV respectively) [14]. It was observed that the value for the wild-type protein was 6 mV more oxidizing than the previously reported value (−198 mV) [23], a difference which was rationalized by the fact that the latter measurement was performed on the C65Y variant of Grx3 (the same variant as used in the present study). Thus it is expected that the M43V/C65Y mutant used here has a redox potential of −209 mV (−198−11 mV).

To measure the redox potential of the M43V/C65Y mutant, conformational stability measurements of the reduced and oxidized protein were performed. The redox potential of a protein can then be determined on basis of the fact that the stability of a disulfide is related to the conformational stability of a protein [24] via thermodynamic linkage (Figure 2). The stabilities of the reduced ($\Delta G^{red}_{H_2O}$) and oxidized ($\Delta G^{ox}_{H_2O}$) mutants were determined to be -3.01 ± 0.04 and -2.55 ± 0.06 kcal · mol^{-1} respectively (Figure 2 and Table 1). Assuming that the Gibbs free energy of disulfide bond formation in the unfolded state of Grx3(M43V/C65Y) is identical with the wild-type ($\Delta G^{SSbond}_U = -1.01$ kcal · mol^{-1} [23]), a value of −1.47 kcal · mol^{-1} is calculated for the Gibbs free energy of disulfide bond formation in the native state (ΔG^{SSbond}_N, i.e. redox potential) using thermodynamic linkage (Figure 2) and the relationship $\Delta G^{o\prime} = -nF\Delta E^{o\prime}$, where n represents the two electrons transferred in this reaction, and F is the Faraday constant 23061 cal · mol^{-1} · V^{-1} [2]. Applying the standard state glutathione reference of −240 mV, this value amounts to a redox potential value of −208 mV, which agrees closely with the calculated value (−209 mV). Thus we have confirmed using thermodynamic cycles that the M43V mutation turns Grx3 into a 10–11 mV more reducing protein and that the C65Y mutation increases the redox potential by 6 mV.

The M43V mutation has an impact on the overall Grx3 tertiary structure

To examine whether the altered activity of the Grx3(M43V) mutant [13,14] can be rationalized in terms of structural changes, both wild-type and the M43V/C65Y variant of Grx3 were probed by CD spectroscopy. CD wavelength scans were collected in both the far- and near-UV regions to probe the secondary and tertiary structures respectively. As seen in Figure 3, the far-UV CD scans demonstrate that all Grx3 protein constructs (as well as the Grx1 ones) have essentially the same secondary structure content. On the other hand, the near-UV scans reveal distinct differences as

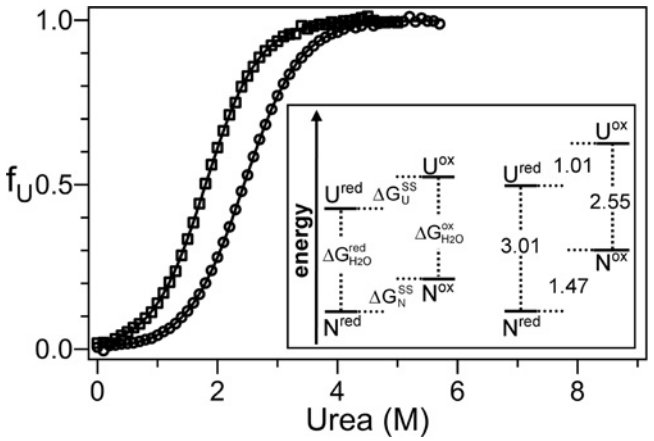

Figure 2 Stability of reduced and oxidized Grx3(M43V/C65Y) monitored by CD spectroscopy

Urea unfolding curves of reduced (○) and oxidized (□) Grx3(M43V/C65Y), monitored by CD spectroscopy at 222 nm. For graphical comparison, the raw CD signal was converted into fraction unfolded protein (f_u). The inset shows a thermodynamic linkage analysis based on the relative Gibbs energies for native (N) and unfolded (U) redox states of a protein on the left. To the right, the analysis applied on Grx3(M43V/C65Y). The Gibbs free energy of disulfide bond formation in the unfolded state (1.01 kcal · mol^{-1}) is assumed to be identical with the wild-type protein.

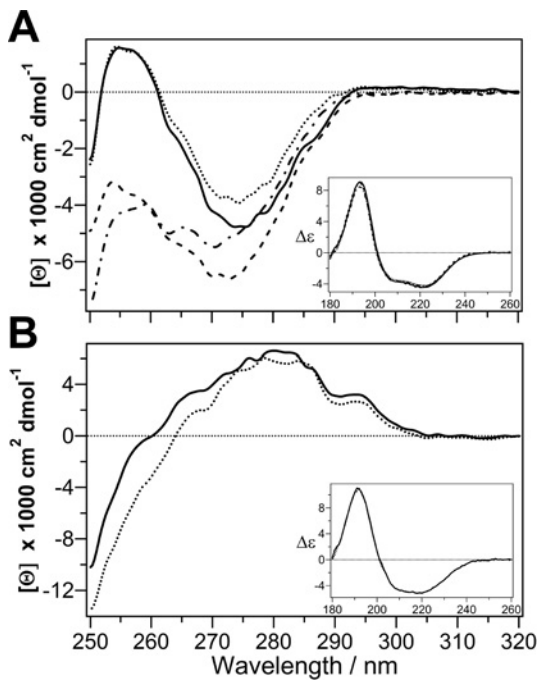

Figure 3 Structural differences between various mutant forms of Grx1 and Grx3 as probed by CD spectroscopy

Smoothed near-UV CD spectra of reduced Grx1 and Grx3 are shown. The insets depict far-UV CD spectra of each protein with the units of $\Delta\varepsilon$ in M^{-1} · cm^{-1}. (**A**) Spectra of wild-type Grx3 (solid line), M43V/C65Y (dotted line), C14S (broken line) and the C14S/M43V/C65Y mutant (broken/dotted line). (**B**) Spectra of wild-type Grx1 (solid line) and its C14S mutant (dotted line).

the M43V mutation results in a more positive ellipticity in the region of 265–280 nm. Differences at these wavelengths reflect a change in the chemical environments of the six aromatic chromophores (four tyrosine and two phenylalanine residues). This could be taken either as an indication that the overall tertiary structure of Grx3 is slightly altered or that some aromatic

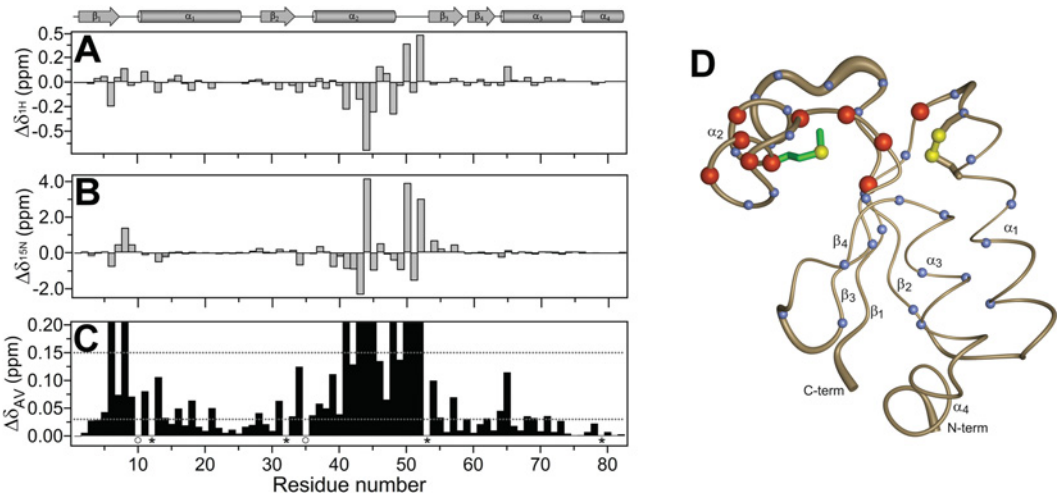

Figure 4 Chemical shift deviations between Grx3 wild-type and M43V/C65Y mutant

Chemical shift deviations ($\Delta\delta_{1H/15Nmut} - \Delta\delta_{1H/15Nwt}$), from two-dimensional ^{1}H-^{15}N HSQC spectra of Grx3 wild-type and M43V/C65Y mutant, plotted as a function of residue number. The secondary structure of wild-type Grx3 [30] is presented above the graphs. The resonances from prolines (*) and Ala^{1}, Thr^{10} and Gly^{35} (○) were not observed in the spectra from both wild-type and mutant Grx3. (**A**) ^{1}H chemical shift deviations. (**B**) ^{15}N deviations. (**C**) Weighted chemical shift deviations accounting for both backbone proton and nitrogen resonances were calculated using the formula $\Delta\delta_{AV} = [0.5(\delta_{Hmut} - \delta_{Hwt})^2 + 0.02(\delta_{Nmut} - \delta_{Nwt})^2]^{\frac{1}{2}}$ [35] and categorized into large ($0.03 < \Delta\delta_{AV} < 0.15$ p.p.m.), and extensive ($\Delta\delta_{AV} \geqslant 0.15$ p.p.m.) chemical shift perturbations as indicated by dotted grey lines. For graphical purposes, the graph has been cut at $\Delta\delta_{AV} = 0.2$ p.p.m. (**D**) Large (blue balls) and extensive (red balls) chemical shift perturbations mapped on to the oxidized wild-type Grx3 structure.

chromophores change from a restrictive and spectroscopically anisotropic environment to a more open and isotropic one, allowing the aromatic rings to flip, as would be expected from a more open and dynamic state. Both Tyr^{6} and Phe^{56} are in close proximity to Met^{43} and a point mutation at this position will most probably alter the chemical environment of these two residues and hence the observed spectral differences may reflect changes in the immediate chemical surrounding of Tyr^{6} and Phe^{56} and not any overall structural alterations.

The structural effect of the M43V mutation has long-range consequences

NMR spectroscopy is capable of providing detailed information on many levels of structure, from three-dimensional structures at atomic resolution to specific chemical environments of a given atom, provided that sequence-specific resonance assignments are known. As the assignment of reduced wild-type Grx3 has been determined within our laboratory ([15] and J. Sagemark, P. Güntert and K.D. Berndt, unpublished work), we set out to obtain the ^{1}H, ^{13}C and ^{15}N assignments of reduced Grx3(M43V/C65Y) in order to compare structural and dynamic features. To achieve the assignment of reduced Grx3(M43V/C65Y), a series of standard triple-resonance experiments were collected. The subsequent analysis was performed semi-automatically using the GARANT program [34] and confirmed manually. In all spectra, Ala^{1}, Thr^{10} and Gly^{35} are missing, an observation made previously for the wild-type protein [15]. As a first assessment of the structural similarity of the two proteins, two-dimensional ^{1}H-^{15}N HSQC spectra were obtained for both wild-type and M43V/C65Y mutant Grx3 proteins. Grx3 contains 78 non-proline residues and a total of 75 backbone amide peaks were observed in each of the wild-type and M43V/C65Y spectra. An unexpectedly large number of resonances were shifted relative to the wild-type protein due to the M43V mutation.

The ^{1}H and ^{15}N chemical shift deviations ($\Delta\delta$) are shown in Figures 4(A) and 4(B) respectively. To account for both ^{1}H and ^{15}N deviations in a single parameter, a weighted statistic (Figure 4C) was calculated using the formula $\Delta\delta_{AV} = [0.5(\delta_{Hmut} - \delta_{Hwt})^2 + 0.02(\delta_{Nmut} - \delta_{Nwt})^2]^{\frac{1}{2}}$ [35]. A total of 41 out of 74 resonances (not including Val[43]) have experienced significant chemical shift deviations ($\Delta\delta_{AV} > 0.03$ p.p.m.) in the mutant protein; nine of these have been subjected to extensive deviations ($\Delta\delta_{AV} \geqslant 0.15$ p.p.m., Figure 4C). It is not surprising that many of these residues are located in the vicinity of Val^{43} (as discussed above) of the mutant protein; however, residues close to the active site (e.g. Lys^{8}, Thr^{51} and Val^{52}) have also experienced extensive deviations (Figure 4D). Interestingly, results from molecular dynamics simulations of wild-type and mutant Grx3 [14] indicate that Lys^{8} and Val^{52} are closer to S$^{\gamma}$ of Cys^{11} in the mutant protein, making direct and water-mediated hydrogen bonds to this thiolate possible. These extra hydrogen bonds in Grx3(M43V/C65Y) would contribute to the reduced pK_a of S$^{\gamma}$ of Cys^{11} (wild-type and mutant proteins have pK_a values of 4.9 and 3.8 respectively), affecting the nucleophilic property and enhancing the leaving group ability of the thiolate of this side chain [36]. A total of 32 residues have backbone amides experiencing large chemical shift perturbations ($0.03 < \Delta\delta_{AV} < 0.15$ p.p.m.). The positions of these residues are spread over the entire protein. It appears as if the M43V mutation has an impact on residues throughout the Grx3 molecule, not only in residues in the vicinity of the mutation.

NMR H/D exchange provides insight of increased slow time-scale motion

The observed differences between the wild-type Grx3 and the M43V/C65Y mutant can be a consequence of tertiary structural rearrangements. However, these results may also be rationalized by differences in main-chain and side-chain dynamics. To probe the slow time-scale motions of proteins, time-resolved H/D backbone amide exchange monitored by NMR has proven to be a useful method [28]. There is evidence that factors limiting amide hydrogen exchange includes the involvement of the amide in a hydrogen bond as well as the solvent accessibility of the amide. Amides participating in secondary structural elements buried inside the

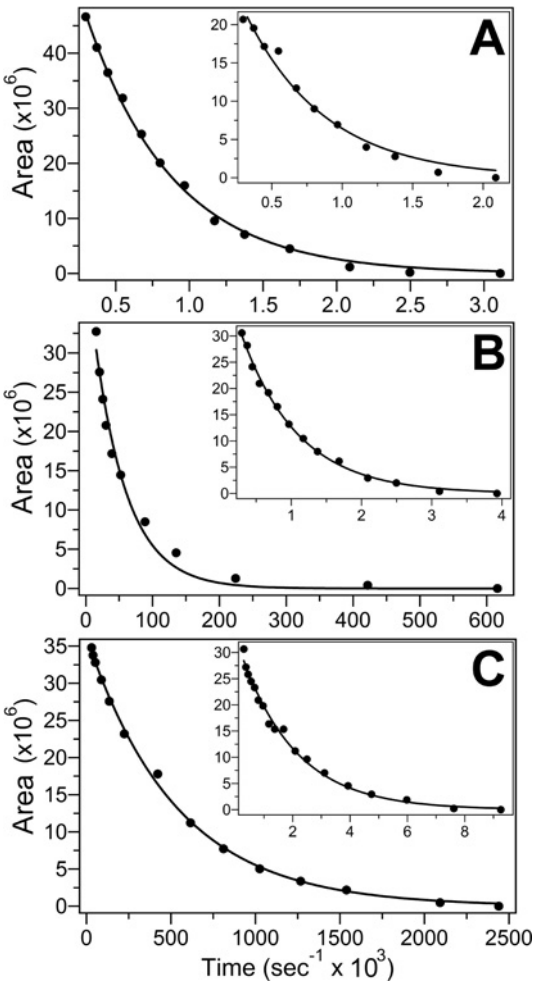

Figure 5 Representative NMR H/D exchange plots

Examples of H/D exchange plots of (**A**) Val^{26}, (**B**) Ser^{22} and (**C**) Glu^{4} exhibiting fast (1.70 ± 0.04 ms), intermediate (17.71 ± 1.37 μs) and slow (1.93×0.06 μs) rates respectively. The insets show the respective plots from the M43V/C65Y mutant with rates of 2.27 ± 0.11 (Val^{26}), 1.23 ± 0.03 (Ser^{22}) and 0.47 ± 0.03 (Glu^{4}) ms^{-1}.

protein are then expected to experience slower exchange with solvent than amides not involved in hydrogen bonds or located on the surface. However, a protein is constantly in a state of flux, populating the thermodynamically and kinetically allowed states. The rate of exchange of a particular amide is related to how frequently it accesses more solvent-exposed conformations, which is an indirect measure of the motional freedom of that amide [28].

The H/D exchange reaction (Figure 5) of the wild-type and M43V/C65Y mutant backbone amides were followed by collecting a series of ^{15}N HSQC spectra at different time points after the addition of $^{2}H_2O$. As shown in Figure 6(A), the H/D exchange reaction was monitored for a total of 42 backbone amides of the wild-type protein, whereas only 34 backbone amides were characterized in the M43V/C65Y mutant. Remarkably, although residual amide protons in the wild-type protein were visible for more than 28 days, there were no detectable peaks from the M43V/C65Y mutant after approx. 6 h. These observations indicate a structurally more rigid wild-type protein, also observed when comparing the conformational stabilities between Grx3 molecules with and without the M43V mutation differing by 2.68 ± 0.14 kcal $\cdot$ mol^{-1} [Grx3(C14S) $= -4.74 \pm 0.12$ and Grx3(C14S/M43V/C65Y) $= -2.06 \pm 0.08$ kcal $\cdot$ mol^{-1}). To be able to correctly assign peaks with fast exchange, shorter NMR experiments were initially used, which had poorer spectral resolution. Consequently, five (out of 42) and four (out of 34) peaks in the wild-type and M43V/C65Y mutant spectra respectively, could not be distinguished due to chemical shift degeneracy. Nevertheless, when comparing the ratios of H/D exchange rates between the wild-type and mutant protein, drastic differences are observed. As shown in Figure 6(B), 26 residues (not counting those with degenerate chemical shifts) experience somewhat faster dynamics ($k_{M43V/C65Y}/k_{WT} < 50$). These residues are not confined to a particular area but are spread throughout the Grx3 molecule (Figure 6C). A total of six residues (not including Met/Val^{43}) have faster dynamics ($50 < k_{M43V/C65Y}/k_{WT} < 150$), whereas eight residues experience much faster dynamics ($k_{M43V/C65Y}/k_{WT} > 150$) in the mutant protein. Interestingly, in contrast with the residues experiencing somewhat faster dynamics, residues having much faster dynamics (except Lys^{18}) are confined to the central β-sheet core buried inside the protein. These results demonstrate that the M43V mutation not only has a striking effect on the central β-sheet core of the Grx3 molecule, but also a global effect on the molecule, increasing the rate at which the structure fluctuates between buried and more solvent-exposed conformations where amide exchange can occur.

It has been argued previously that the apparent substrate promiscuity of Grx1 might be due to a higher degree of 'dynamic plasticity' [16] as it exhibits a more 'open' structure compared with Grx3 in the area of the active site [14]. The data presented above provide the first direct experimental evidence that the M43V mutation in Grx3 results in a protein with a greater conformational flexibility. Initial biochemical data investigating the Grx1-like behaviour of the Grx3(M43V/C65Y) mutant concluded that an increased V_{max} and not K_m in conjunction with a lowered active site cysteine residue redox potential (by 11 mV) and a lowered pK_a (by 0.9 unit) of the N-terminal active site cysteine residue was responsible for the altered activity [14]. Our results from the present study confirm the lower active site redox potential caused by the M43V mutation. However, in contrast with Porat et al. [14], we demonstrate that the Grx3(M43V/C65Y) mutant has acquired a Grx1-like affinity for RR not present in wild-type Grx3. Although there were no detectable secondary structural perturbations as probed by far-UV CD spectroscopy, both near-UV CD and NMR ^{1}H-^{15}N correlation data demonstrate that there are differences between the wild-type and M43V/C65Y mutant Grx3. These differences could be the result of changes in tertiary structure; however, the H/D exchange measurements point to distinct patterns of residues with dramatically altered behaviour where the M43V mutation has had a global effect on the protein, causing the mutant to more frequently access an exposed structure. The lower conformational stability (by 2.68 ± 0.14 kcal $\cdot$ mol^{-1}) of the mutant protein compared with the wild-type is also an indication that a greater population of exposed molecules is expected in the M43V/C65Y mutant. The Met^{43} side chain is buried under the second helix in Grx3, where it makes many contacts to surrounding residues. Replacing this methionine residue with an amino acid containing a smaller or branched side chain could disrupt the inner core, leaving the protein with fewer contacts between these structural units and a greater motional freedom. This increased freedom could be responsible for accommodating a wider variety of substrates. Whether this molecular transformation is a theme found in other proteins remains to be seen. However, multiple sequence alignment [2] reveals that dithiol Grxs in general have various hydrophobic residues in the corresponding Grx3 Met^{43} position, suggesting that this may be a strategy to facilitate substrate promiscuity within this family of proteins. Finally, whether alterations in dynamics alone are responsible for

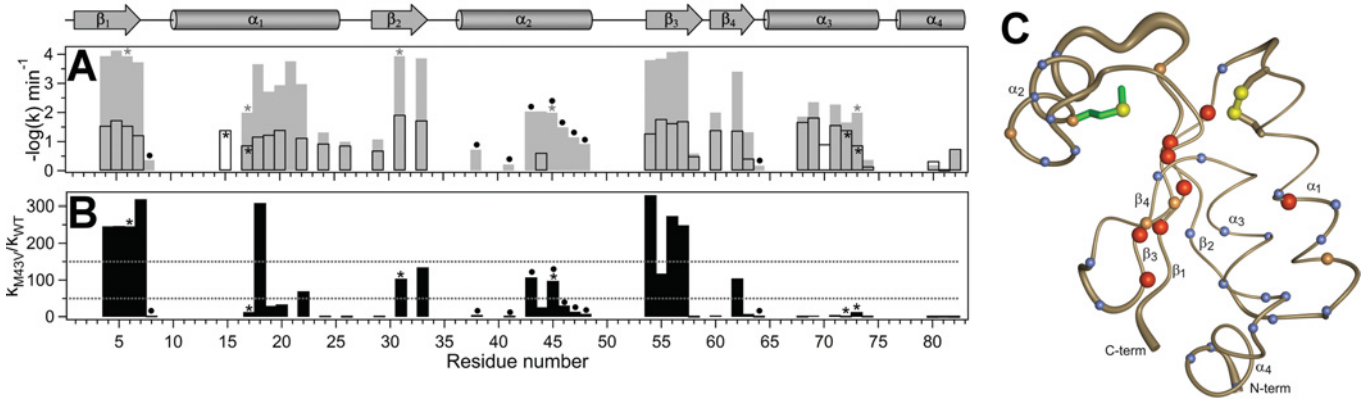

Figure 6 Plot of H/D exchange rate values against residue number

(**A**) Plot of $-\log(k)$ values of wild-type Grx3 (filled grey boxes) and its M43V/C65Y mutant (black boxes). Grey and black asterisks indicate uncertainty due to peak overlap in the wild-type and M43V/C65Y spectra respectively. A filled black circle indicates backbone amides that, in contrast with the wild-type protein, could not be detected within the timeframe of the NMR measurement. (**B**) Ratios of the M43V/C65Y mutant and wild-type rate constants. Here a black asterisk indicates an uncertain value due to peak overlap, whereas a filled black circle indicates that the ratio is based on a k value of 1 s^{-1} for the M43V/C65Y mutant. Grey dotted lines separate residues of the M43V/C65Y mutant with slightly faster ($k_{M43V/C65Y}/k_{WT} < 50$), faster (between 50 and 150) and much faster (>150) H/D exchange rates than the wild-type protein. In (**C**), the residues representing the slightly faster (blue balls), faster (brown balls), and much faster (red balls) H/D exchange rates have been mapped out on the oxidized wild-type Grx3 structure [30]. The secondary structure of the oxidized wild-type Grx3 is shown above the graphs.

the change in activity or if structural alterations also are involved is the subject of ongoing research, part of which includes the structure determination of the Grx3(M43V/C65Y) mutant using NMR.

AUTHOR CONTRIBUTION

This study is the result of collaboration between the laboratories of Kurt Berndt and Jon Beckwith. The planning of the majority of experiments contained in this work was carried out by Kurt Berndt and Tobias Elgán, the latter being the primary person who performed the experiments described in the present study. The *in vivo* activity measurements were planned and conducted by Anne-Gaëlle Planson and Jon Beckwith. The automated NMR data processing performed using the software package GARANT was supervised by Peter Güntert. Tobias Elgán was primarily responsible for writing the manuscript under the supervision of Kurt Berndt. All authors read and made comments on the paper prior to submission.

FUNDING

This work was supported by the Karolinska Institutet and Södertörns Högskola (to K.D.B.), the National Institutes of Health [grant number GMO41883 (to J.B.)], and the Scandinavia-Japan Sasakawa Foundation and the Boehringer Ingelheim Fonds (to T.H.E.). J.B. is an American Cancer Society Professor. P.G. is supported by the Volkswagen Foundation and by a Grant-in-Aid for Scientific Research of the Japan Society for the Promotion of Science.

REFERENCES

1 Martin, J. L. (1995) Thioredoxin–a fold for all reasons. Structure **3**, 245–250
2 Sagemark, J., Elgán, T. H., Bürglin, T. R., Johansson, C., Holmgren, A. and Berndt, K. D. (2007) Redox properties and evolution of human glutaredoxins. Proteins **68**, 879–892
3 Åslund, F. and Beckwith, J. (1999) Bridge over troubled waters: sensing stress by disulfide bond formation. Cell **96**, 751–753
4 Shelton, M. D., Chock, P. B. and Mieyal, J. J. (2005) Glutaredoxin: role in reversible protein S-glutathionylation and regulation of redox signal transduction and protein translocation. Antioxid. Redox Signaling **7**, 348–366
5 Gallogly, M. M., Starke, D. W. and Mieyal, J. J. (2009) Mechanistic and kinetic details of catalysis of thiol-disulfide exchange by glutaredoxins and potential mechanisms of regulation. Antioxid. Redox Signaling **11**, 1059–1081
6 Bushweller, J. H., Åslund, F., Wüthrich, K. and Holmgren, A. (1992) Structural and functional characterization of the mutant *Escherichia coli* glutaredoxin (C14/S) and its mixed disulfide with glutathione. Biochemistry **31**, 9288–9293
7 Fernandes, A. P. and Holmgren, A. (2004) Glutaredoxins: glutathione-dependent redox enzymes with functions far beyond a simple thioredoxin backup system. Antioxid. Redox Signaling **6**, 63–74
8 Nordstrand, K., Åslund, F., Holmgren, A., Otting, G. and Berndt, K. D. (1999) NMR structure of *Escherichia coli* glutaredoxin 3-glutathione mixed disulfide complex: implications for the enzymatic mechanism. J. Mol. Biol. **286**, 541–552
9 Vlamis-Gardikas, A., Åslund, F., Spyrou, G., Bergman, T. and Holmgren, A. (1997) Cloning, overexpression, and characterization of glutaredoxin 2, an atypical glutaredoxin from *Escherichia coli*. J. Biol. Chem. **272**, 11236–11243
10 Åslund, F., Ehn, B., Miranda-Vizuete, A., Pueyo, C. and Holmgren, A. (1994) Two additional glutaredoxins exist in *Escherichia coli*: glutaredoxin 3 is a hydrogen donor for ribonucleotide reductase in a thioredoxin/glutaredoxin 1 double mutant. Proc. Natl. Acad. Sci. U.S.A. **91**, 9813–9817
11 Prinz, W. A., Åslund, F., Holmgren, A. and Beckwith, J. (1997) The role of the thioredoxin and glutaredoxin pathways in reducing protein disulfide bonds in the *Escherichia coli* cytoplasm. J. Biol. Chem. **272**, 15661–15667
12 Lillig, C. H., Prior, A., Schwenn, J. D., Åslund, F., Ritz, D., Vlamis-Gardikas, A. and Holmgren, A. (1999) New thioredoxins and glutaredoxins as electron donors of 3′-phosphoadenylylsulfate reductase. J. Biol. Chem. **274**, 7695–7698
13 Ortenberg, R., Gon, S., Porat, A. and Beckwith, J. (2004) Interactions of glutaredoxins, ribonucleotide reductase, and components of the DNA replication system of *Escherichia coli*. Proc. Natl. Acad. Sci. U.S.A. **101**, 7439–7444
14 Porat, A., Lillig, C. H., Johansson, C., Fernandes, A. P., Nilsson, L., Holmgren, A. and Beckwith, J. (2007) The reducing activity of glutaredoxin 3 toward cytoplasmic substrate proteins is restricted by methionine 43. Biochemistry **46**, 3366–3377
15 Åslund, F., Nordstrand, K., Berndt, K. D., Nikkola, M., Bergman, T., Ponstingl, H., Jörnvall, H., Otting, G. and Holmgren, A. (1996) Glutaredoxin-3 from *Escherichia coli*. Amino acid sequence, ^{1}H and ^{15}N NMR assignments, and structural analysis. J. Biol. Chem. **271**, 6736–6745
16 Berardi, M. J. and Bushweller, J. H. (1999) Binding specificity and mechanistic insight into glutaredoxin-catalyzed protein disulfide reduction. J. Mol. Biol. **292**, 151–161
17 Elgán, T. H. and Berndt, K. D. (2008) Quantifying *E. coli* glutaredoxin-3 substrate specificity using ligand-induced stability. J. Biol. Chem. **283**, 32839–32847
18 Marley, J., Lu, M. and Bracken, C. (2001) A method for efficient isotopic labeling of recombinant proteins. J. Biomol. NMR **20**, 71–75
19 Gill, S. C. and von Hippel, P. H. (1989) Calculation of protein extinction coefficients from amino acid sequence data. Anal. Biochem. **182**, 319–326
20 Berardi, M. J., Pendred, C. L. and Bushweller, J. H. (1998) Preparation, characterization, and complete heteronuclear NMR resonance assignments of the glutaredoxin (C14S)-ribonucleotide reductase B1 737–761 (C754S) mixed disulfide. Biochemistry **37**, 5849–5857
21 Pace, C. N. and Scholtz, M. (1997), Measuring the conformational stability of a protein. In Protein Structure: a Practical Approach, 2nd edition (Creighton, T.E., ed.) pp. 299–321, Oxford University Press, Oxford
22 Santoro, M. M. and Bolen, D. W. (1988) Unfolding free energy changes determined by the linear extrapolation method. 1. Unfolding of phenylmethanesulfonyl α-chymotrypsin using different denaturants. Biochemistry **27**, 8063–8068

23 Åslund, F., Berndt, K. D. and Holmgren, A. (1997) Redox potentials of glutaredoxins and other thiol-disulfide oxidoreductases of the thioredoxin superfamily determined by direct protein-protein redox equilibria. J. Biol. Chem. **272**, 30780–30786
24 Lin, T. Y. and Kim, P. S. (1989) Urea dependence of thiol-disulfide equilibria in thioredoxin: confirmation of the linkage relationship and a sensitive assay for structure. Biochemistry **28**, 5282–5287
25 Bax, A. (1994) Multidimensional nuclear magnetic resonance methods for protein studies. Curr. Opin. Struct. Biol. **4**, 738–744
26 Delaglio, F., Grzesiek, S., Vuister, G. W., Zhu, G., Pfeifer, J. and Bax, A. (1995) NMRPipe: a multidimensional spectral processing system based on UNIX pipes. J. Biomol. NMR **6**, 277–293
27 Bartels, C., Billeter, M., Güntert, P. and Wüthrich, K. (1996) Automated sequence-specific NMR assignment of homologous proteins using the program GARANT. J. Biomol. NMR **7**, 207–213
28 Dempsey, C. E. (2001) Hydrogen exchange in peptides and proteins using NMR spectroscopy. Prog. Nucl. Magn. Reson. Spectrosc. **39**, 135–170
29 Bartels, C., Xia, T., Billeter, M., Güntert, P. and Wüthrich, K. (1995) The program XEASY for computer-supported NMR spectral analysis of biological macromolecules. J. Biomol. NMR **6**, 1–10
30 Nordstrand, K., Sandström, A., Åslund, F., Holmgren, A., Otting, G. and Berndt, K. D. (2000) NMR structure of oxidized glutaredoxin 3 from *Escherichia coli*. J. Mol. Biol. **303**, 423–432
31 Tamarit, J., Belli, G., Cabiscol, E., Herrero, E. and Ros, J. (2003) Biochemical characterization of yeast mitochondrial Grx5 monothiol glutaredoxin. J. Biol. Chem. **278**, 25745–25751
32 Saaranen, M. J., Salo, K. E., Latva-Ranta, M. K., Kinnula, V. L. and Ruddock, L. W. (2009) The C-terminal active site cysteine of *Escherichia coli* glutaredoxin 1 determines the glutathione specificity of the second step of peptide deglutathionylation. Antioxid. Redox Signaling **11**, 1819–1828
33 Reference deleted
34 Bartels, C., Güntert, P., Billeter, M. and Wüthrich, K. (1997) GARANT - a general algorithm for resonance assignment of multidimensional nuclear magnetic resonance spectra. J. Comp. Chem. **18**, 139–149
35 Grzesiek, S., Stahl, S. J., Wingfield, P. T. and Bax, A. (1996) The CD4 determinant for downregulation by HIV-1 Nef directly binds to Nef. Mapping of the Nef binding surface by NMR. Biochemistry **35**, 10256–10261
36 Shaked, Z., Szajewski, R. P. and Whitesides, G. M. (1980) Rates of thiol-disulfide interchange reactions involving proteins and kinetic measurements of thiol pKa values. Biochemistry **19**, 4156–4166

Received 23 February 2010/24 June 2010; accepted 6 July 2010
Published as BJ Immediate Publication 6 July 2010, doi:10.1042/BJ20100289